



Presence versus Proximity: The Role of Pendant Amines in the Catalytic Hydrolysis of a Nerve Agent Simulant

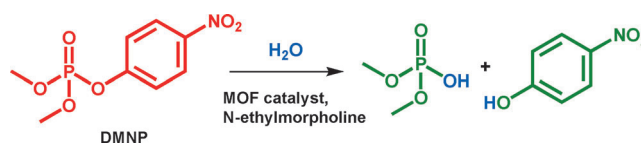
Timur Islamoglu, Manuel A. Ortuño, Emmanuel Proussaloglou, Ashlee J. Howarth, Nicolaas A. Vermeulen, Ahmet Atilgan, Abdullah M. Asiri, Christopher J. Cramer, and Omar K. Farha*

Abstract: Amino-functionalized zirconium-based metal-organic frameworks (MOFs) have shown unprecedented catalytic activity compared to non-functionalized analogues for hydrolysis of organophosphonate-based toxic chemicals. Importantly, the effect of the amino group on the catalytic activity is significantly higher in the case of UiO-66-NH₂, where the amino groups reside near the node, compared to UiO-67-m-NH₂, where they are directed away from the node. Herein, we show that the proximity of the amino group is crucial for fast catalytic activity towards hydrolysis of organophosphonate-based nerve agents. The generality of the observed amine-proximity-dictated catalytic activity has been tested on two different MOF systems which have different topology. DFT calculations reveal that amino groups on all the MOFs studied are not acting as Brønsted bases; instead they control the microsolvation environment at the Zr₆-node active site and therefore increase the overall catalytic rates.

Nerve agents are organophosphonate compounds that inhibit acetylcholinesterase (AChE)-an enzyme responsible for the breakdown of neurotransmitters.^[1] Organophosphonate-based nerve agents bind covalently to the esteratic site of AChE resulting in a build-up of neurotransmitters, which leads to muscle fasciculation and eventual death by asphyxiation.^[2] Although the production, stockpiling, and use of chemical weapons has been banned by an international convention,^[3] there are still reports of chemical warfare agents, including nerve agents, being used today.^[4] Developing materials for the simple and fast abatement of these toxic chemicals therefore remains a very important challenge. In regards to nerve agent detoxification, selective hydrolysis of

the P–F bond found in nerve agents, such as Sarin and Soman, has been shown to be effective for mitigating toxicity.^[5] While a number of different metal oxides are capable of catalyzing the hydrolysis of this P–F bond, the development of advanced materials, and specifically catalysts capable of further enabling this reaction, are still needed.^[6]

Metal–organic frameworks (MOFs) are self-assembled, and atomically precise porous materials comprising metal ions/clusters and organic linkers.^[7] MOFs have been employed as catalysts and catalyst supports, in part because of their ordered nature, structural tunability, and permanent porosity.^[8] We and others have shown that fine-tuning pore size,^[9] particle size,^[10] metal node connectivity^[11] and chemical composition^[12] can favorably affect the activity of MOF-based catalysts in the hydrolysis of a nerve agent simulant, dimethyl 4-nitrophenyl phosphate (DMNP). Importantly, DMNP has been shown to be effective for mimicking the reactivity of organophosphonate-based nerve agents (Scheme 1).^[13]



Scheme 1. Hydrolysis reaction of phosphonate-based nerve agent simulant (dimethyl 4-nitrophenyl phosphonate, DMNP).

Among the linker-appended functional groups screened, primary amine bearing MOFs have shown unprecedented activity in the hydrolysis of DMNP. We have demonstrated that, while keeping other factors constant, installing a primary amine group on the benzene-1,4-dicarboxylic acid (BDC) linkers of UiO-66 (Figure 1) can accelerate the catalytic hydrolysis of DMNP by 20 times compared to the parent UiO-66 (Figure 2 and Table 1).^[12a] We originally attributed this activity to synergistic effects between the amine group on the linker and the Zr^{IV} node which could act as a proximal base and Lewis acid, respectively. We hypothesized that this synergy would result in enhanced catalytic activity towards phosphate ester bond hydrolysis since the phosphotriesterase enzyme that performs this reaction in nature also contains a Lewis acidic active site with a proximal base. In addition to the promising activity demonstrated by UiO-66 and its amino functionalized derivative, we have also shown that using UiO-67 (Figure 1), a MOF which is isostructural to UiO-66 but contains 4,4'-biphenyldicarboxylic acid linkers and larger pores, results in a further enhancement in hydrolysis reaction

*] Dr. T. Islamoglu, E. Proussaloglou, Dr. A. J. Howarth, Dr. N. A. Vermeulen, A. Atilgan, Prof. O. K. Farha
Department of Chemistry
Northwestern University
2145 Sheridan Road, Evanston, IL 60208-3113 (USA)
E-mail: o-farha@northwestern.edu

Dr. M. A. Ortuño, Prof. C. J. Cramer
Department of Chemistry, Supercomputing Institute, and Chemical Theory Center, University of Minnesota
Minneapolis, MN 55455 (USA)
Prof. A. M. Asiri, Prof. O. K. Farha
Department of Chemistry, Faculty of Science King Abdulaziz, University Jeddah
Jeddah 21589 (Saudi Arabia)

Supporting information and the ORCID identification number(s) for the author(s) of this article can be found under:
<https://doi.org/10.1002/anie.201712645>.

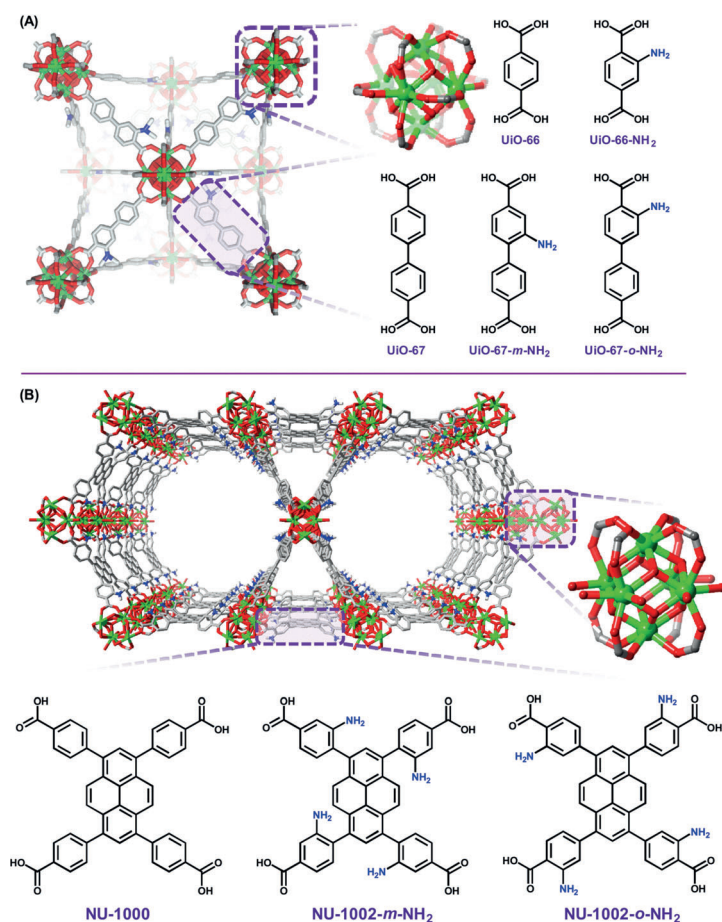


Figure 1. A) Structural representation of UiO-67-*o*-NH₂ and linkers for UiO-66 and UiO-67 series MOFs. B) Structural representation of NU-1002-*o*-NH₂ and linkers for NU-1000 series MOFs (*m* = *meta*, *o* = *ortho*).

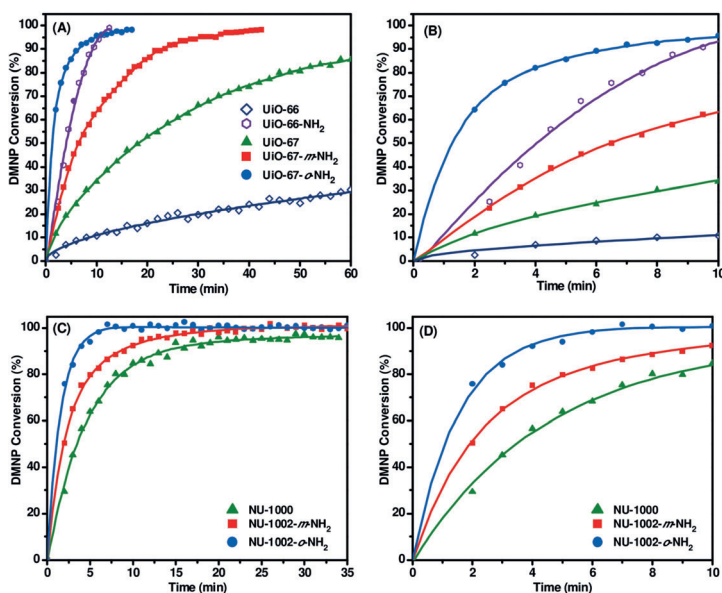


Figure 2. A)–D) Hydrolysis profile of DMNP with UiO-66, UiO-67 and NU-1000 series MOFs using 3 mol% catalyst loading. B) and D) are the same conversion profiles as (A) and (C), respectively, expanding the first 10 min for clarity. See Experimental Section in the Supporting Information for details of reaction conditions.

rate compared to UiO-66 (Figure 2 and Table 1).^[9,12a] This reaction rate enhancement is to be expected given that diffusion of the simulant DMNP in UiO-67 is expected to be faster compared to that in UiO-66.^[14] Since primary amines have been shown to have a favorable effect on DMNP hydrolysis and the apertures of UiO-67 are known to promote DMNP diffusion, the next step was to test the activity of amine functionalized UiO-67 against DMNP. It should be noted that we previously tested the activity of UiO-67-*m*-NH₂ for DMNP hydrolysis at a catalyst loading of 6 mol%. Herein we chose to use 3 mol% catalyst loading since at lower catalyst loading more data points can be collected before DMNP is consumed giving rise to a more accurate conversion versus time profile. As found previously at higher catalyst loadings, we observe enhanced activity for UiO-67-*m*-NH₂ compared to UiO-67 where the half-life for DMNP conversion dropped from 17.9 min to 6.8 min (Table 1 and Figure 2). At these same catalyst loadings (3 mol%), the incorporation of primary amines has a much more drastic effect on the activity of UiO-66 where the half-life decreased from 63.5 min to 3.1 min from UiO-66 to UiO-66-NH₂, respectively. Given that both UiO-66-NH₂ and UiO-67-*m*-NH₂ contain an aromatic amine with comparable pK_a value, the difference between the catalytic activity of these two MOFs must be more than simply a buffering effect. Thus, we turned our attention to the active site of our catalyst—the Zr₆ cluster node of the MOF. The major difference in the chemical environment surrounding the active site of each MOF is that the NH₂ group resides in the vicinity of the node in the case of UiO-66-NH₂ while it is directed away from the node in the case of UiO-67-*m*-NH₂ (Figure 1). It is well-documented that the chemical and/or physical environment around a catalyst active site can have significant effects on catalytic rates.^[15] Therefore, we speculated that the effect of the amine group in UiO-67-*m*-NH₂ is less pronounced compared to UiO-66-NH₂ due to the proximity of the amine to the Zr₆ node in UiO-66-NH₂. To test this hypothesis, we synthesized UiO-67-*o*-NH₂ where the amine is in close proximity to the node as in the case of UiO-66-NH₂. Hydrolysis experiments confirmed our hypothesis where an almost four-fold enhancement in catalytic activity is observed when the amine is located in the *ortho* position of the linker (i.e. closer to the node) versus the *meta* position. Additionally, UiO-67-*o*-NH₂ presents a ten-fold increase in catalytic activity compared to the parent UiO-67. To test the generality of the observed catalytic activity driven by the location of the amine, we have also designed another series of Zr-based MOFs with -NH₂ groups installed in different locations. The new system is based on NU-1000, a MOF with csq-topology containing mesoporous (ca. 30 Å) hexagonal channels and microporous (12 Å) triangular channels connected by 10 Å × 8 Å orthogonal windows which allow for facile diffusion of substrate/product. NU-1002-*o*-NH₂ showed a three-

Table 1: Initial rates and half-lives for MOFs for hydrolysis of DMNP.^[a]

MOFs	Surface Area [m ² g ⁻¹]	Pore Size [Å]	Half-life [min]	Initial Rate [mM s ⁻¹]
UiO-66	1570	10.9/15.9	63.5	0.005
UiO-66-NH ₂	1350	10.9/14.8	3.1	0.093
UiO-67	2400	11.8/21.6	17.9	0.016
UiO-67- <i>m</i> -NH ₂	2020	11.8/21.6	6.8	0.042
UiO-67- <i>o</i> -NH ₂	2050	11.8/21.6	1.8	0.163
NU-1000	2100	11.8/29.5	3.6	0.079
NU-1002- <i>m</i> -NH ₂	1700	12.7/27.3	2.8	0.103
NU-1002- <i>o</i> -NH ₂	1720	12.7/27.4	1.2	0.250

[a] See experimental section in the Supporting Information for details of reaction conditions (*m* = *meta*, *o* = *ortho*).

fold enhancement compared to NU-1000 and more than two-fold enhancement compared to NU-1002-*m*-NH₂ in the catalytic hydrolysis of DMNP (Figure 2 and Table 1). These results emphasize that the observed difference in the catalytic activity is mainly due to the proximity of the amine rather than a simple pore confinement effect. Moreover, the fast hydrolysis rate demonstrated by NU-1002-*o*-NH₂ (*t*_{1/2} = 1.2 min with 3 mol % cat. loading) places it among the best heterogeneous catalysts developed for DMNP hydrolysis.^[5a-b, 6a, 11a, 16] It is worth noting that UiO-67-*o*-NH₂ and NU-1002-*o*-NH₂ present moderate enhancement in catalytic activity compared to UiO-66-NH₂, which can be attributed to a lower local amine concentration around the Zr₆ node in the former. Experimental N₂ adsorption-desorption isotherms, corresponding pore size distribution analysis, and powder X-ray diffraction (PXRD) data confirm the structure of each MOF and that each framework series has comparable BET surface areas while SEM images show comparable particle sizes within the same series of MOF family (Figure S10–S14 in the Supporting Information). Diffuse reflectance infrared Fourier transform spectroscopy (DRIFTS) experiments performed on amine functionalized MOFs show asymmetric and symmetric amino group stretching bands which suggests that free amino groups are present in the MOF (Figure S15). It is important to note that, in homogeneous systems, proximal aromatic amines have been shown to facilitate the delivery of phosphate ester substrates to the nearby catalytic active site via the formation of H-bonds between the amine and phosphate ester.^[17] As a result, significantly faster hydrolysis rates for phosphonate ester species have been achieved by using catalysts bearing amino groups as opposed to their parent structures.^[18]

To reveal the influence of the amino functionality (Table 1), we modeled^[19] the hydrolysis reaction coordinate at the density functional level of theory (DFT) using the M06-L functional (see Supporting Information for details). Although pristine Zr₆ nodes (as in defect-free UiO-66) are fully coordinated with twelve linkers, it is defective nodes with missing linkers that are responsible for catalytic reactivity. From periodic DFT calculations of UiO-66-NH₂^[20] we designed a cluster model with one missing linker to study the local reactivity of the node (Figure S17). To properly account for water solvent, we include four explicit water molecules near the reaction

center with the cluster then surrounded by an implicit solvation model for all optimized species (i.e., a continuum-cluster approach). We emphasize that with these calculations, we aim primarily to describe qualitative trends as quantitative accuracy is necessarily limited in models addressing reactivity at large length and time scales with sizable microsolvation shells. We anticipate the cluster nature of the computational models used for the UiO-66 family to be transferable to UiO-67 analogues and other Zr₆-based MOFs exposing similar reactive sites (e.g., NU-1000^[21] and MOF-808^[22]).

The hydrolysis mechanism entails coordination of DMNP,^[23] water attack at phosphorus, elimination of ArOH, and decoordination of the hydrolyzed product.^[11b, 24] Recent DFT calculations have suggested that water attack is rate determining,^[24a] and so we focus on this step. We consider as zeroes of energy, DMNP bound to a defective node and surrounded by four water molecules. For UiO-66-NH₂, Figure 3 shows the free energies and transition-state (TS) structures for the nucleophilic attack of water. In **TS1** (17.0 kcal mol⁻¹, Figure 3 left), the amino group deprotonates water, forming an incipient nucleophilic hydroxo group that readily attacks the DMNP bound to the node. In lower-energy **TS2**, however (9.5 kcal mol⁻¹, Figure 3 right), the amino group is instead a spectator, and the deprotonation of nearby water is promoted by a hydroxo bound to Zr. For both **TS1** and **TS2**, all three remaining water molecules are in the same position forming an H-bonding network between the amino and μ₃-OH groups. Therefore, the comparison between **TS1** and **TS2** mostly reflects energetic changes associated with the relative basicity of the different proton acceptors. The free energy difference of 7.5 kcal mol⁻¹ favoring **TS2** indicates that the amino group does *not* play a role as a Brønsted base, consistent with the low basicities of anilines in general.^[25] Instead, we infer that the amino groups finely tune the solvent coordination shell around the defect site, thus increasing the nucleophilicity of reacting water molecules.

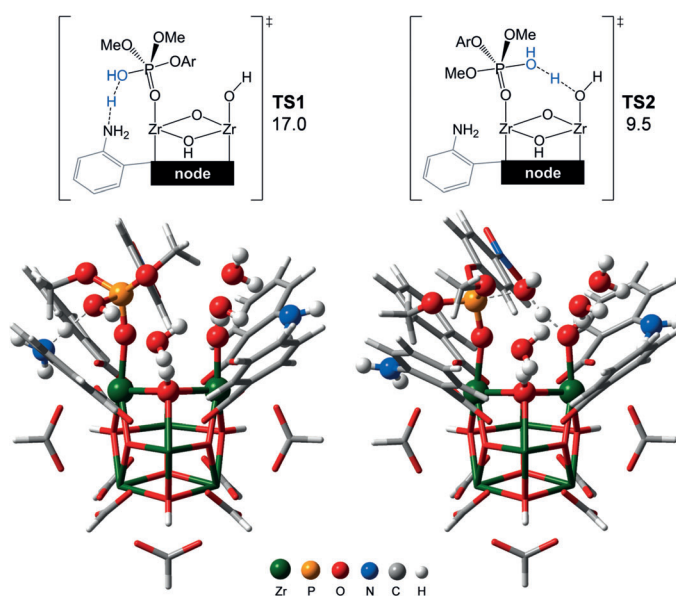


Figure 3. Transition state structures for the water addition step in UiO-66-NH₂. ΔG_{water} in kcal mol⁻¹. ArO = 4-nitrophenoxide.

This indirect effect of amino groups is in line with other recent computational studies in related MOF systems.^[20,26]

To further validate this hypothesis, we investigated the water addition step for UiO-66 and UiO-66-OH. According to previous experimental studies^[12a] the initial rates for hydrolysis follow the trend UiO-66-NH₂ > UiO-66 > UiO-66-OH. In line with experiment, our calculations via corresponding TS2-type transition states predict relative activation free energies of 9.5 (UiO-66-NH₂), 11.3 (UiO-66), and 13.3 (UiO-66-OH) kcal mol⁻¹ (Figure S18). The results presented for UiO-66-NH₂ and UiO-66 relate to those found for UiO-67-*o*-NH₂ and UiO-67 derivatives (Table 1). As for UiO-67-*m*-NH₂, similar although less dramatic effects are expected due to the greater distance between the *meta*-amino substituent and the active site of the node. Modeling UiO-67-*m*-NH₂, however would require the use of a large microsolvation shell such that statistical sampling intractable at the fully quantum mechanical level would become necessary, and thus we have not attempted to address this given the relatively small free energy differences observed experimentally.

In conclusion, we tackled, for the first time, understanding the role of amino functionalities on MOFs for the hydrolysis of a nerve agent simulant. Owing to the tunability of MOFs at the atomic level, we were able to show that not only the presence but also the proximity of the amino group is important for effective chemical detoxification of a phosphate-ester based nerve agent simulant. Our calculations rule out amino groups as Brønsted bases and suggest that more subtle changes in microsolvation around the defect sites likely govern the reactivity trends. Unraveling the mechanistic role of functionalized linkers will help guide the design of more efficient MOF catalysts for nerve agent destruction.

Acknowledgements

O.K.F. gratefully acknowledges support from the Defense Threat Reduction Agency (HDTRA1-18-1-0003) for the catalysis study and Army Research Office-STTR (W911SR-17-C-0007) for the linkers and the MOFs syntheses. C.J.C. acknowledge the US DOE, Office of Basic Energy Sciences, Division of Chemical Sciences, Geosciences and Biosciences (Award DE-FG02-12ER16362) as well as the Minnesota Supercomputing Institute (MSI) at the University of Minnesota for providing resources that contributed to the theoretical modelling results reported within this paper. This work made use of the EPIC, Keck-II, and/or SPID facilities of Northwestern University's NUANCE Center, which has received support from the Soft and Hybrid Nanotechnology Experimental (SHyNE) Resource (NSF ECCS-1542205); the MRSEC program (NSF DMR-1121262) at the Materials Research Center; the International Institute for Nanotechnology (IIN); the Keck Foundation; and the State of Illinois, through the IIN.

Conflict of interest

The authors declare no conflict of interest.

Keywords: amino groups · heterogeneous catalysis · hydrolysis · metal–organic frameworks · nerve agents

- [1] K. Kim, O. G. Tsay, D. A. Atwood, D. G. Churchill, *Chem. Rev.* **2011**, *111*, 5345–5403.
- [2] G. Mercey, T. Verdelet, J. Renou, M. Kliachyna, R. Baati, F. Nachon, L. Jean, P.-Y. Renard, *Acc. Chem. Res.* **2012**, *45*, 756–766.
- [3] Organisation for the Prohibition of Chemical Weapons. Chemical Weapons Convention. <https://www.opcw.org/chemical-weapons-convention/> (accessed August, 2017).
- [4] “The Syrian Government’s Widespread and Systematic Use of Chemical Weapons”: O. Solvang in *Death by Chemicals* (Ed.: S. L. Whitson), Human Rights Watch United States of America, 2017.
- [5] a) Y. Y. Liu, A. J. Howarth, N. A. Vermeulen, S. Y. Moon, J. T. Hupp, O. K. Farha, *Coord. Chem. Rev.* **2017**, *346*, 101–111; b) N. S. Bobbitt, M. L. Mendonca, A. J. Howarth, T. Islamoglu, J. T. Hupp, O. K. Farha, R. Q. Snurr, *Chem. Soc. Rev.* **2017**, *46*, 3357–3385; c) E. Barea, C. Montoro, J. A. Navarro, *Chem. Soc. Rev.* **2014**, *43*, 5419–5430; d) B. M. Smith, *Chem. Soc. Rev.* **2008**, *37*, 470–478.
- [6] a) J. B. DeCoste, G. W. Peterson, *Chem. Rev.* **2014**, *114*, 5695–5727; b) T. J. Bandosz, M. Laskoski, J. Mahle, G. Mogilevsky, G. W. Peterson, J. A. Rossin, G. W. Wagner, *J. Phys. Chem. C* **2012**, *116*, 11606–11614.
- [7] a) H.-C. Zhou, J. R. Long, O. M. Yaghi, *Chem. Rev.* **2012**, *112*, 673–674; b) V. Guillermin, D. Kim, J. F. Eubank, R. Luebke, X. Liu, K. Adil, M. S. Lah, M. Eddaoudi, *Chem. Soc. Rev.* **2014**, *43*, 6141–6172.
- [8] a) H. Furukawa, K. E. Cordova, M. O’Keeffe, O. M. Yaghi, *Science* **2013**, *341*, 1230444; b) T. Islamoglu, S. Goswami, Z. Li, A. J. Howarth, O. K. Farha, J. T. Hupp, *Acc. Chem. Res.* **2017**, *50*, 805–813; c) S. M. J. Rogge, A. Bavykina, J. Hajek, H. Garcia, A. I. Olivos-Suarez, A. Sepulveda-Escribano, A. Vimont, G. Clet, P. Bazin, F. Kapteijn, M. Daturi, E. V. Ramos-Fernandez, F. X. Llabres i Xamena, V. Van Speybroeck, J. Gascon, *Chem. Soc. Rev.* **2017**, *46*, 3134–3184; d) A. Atilgan, T. Islamoglu, A. J. Howarth, J. T. Hupp, O. K. Farha, *ACS Appl. Mater. Interfaces* **2017**, *9*, 24555–24560.
- [9] G. W. Peterson, S.-Y. Moon, G. W. Wagner, M. G. Hall, J. B. DeCoste, J. T. Hupp, O. K. Farha, *Inorg. Chem.* **2015**, *54*, 9684–9686.
- [10] P. Li, R. C. Klet, S.-Y. Moon, T. C. Wang, P. Deria, A. W. Peters, B. M. Klahr, H.-J. Park, S. S. Al-Juaied, J. T. Hupp, O. K. Farha, *Chem. Commun.* **2015**, *51*, 10925–10928.
- [11] a) S. Y. Moon, Y. Liu, J. T. Hupp, O. K. Farha, *Angew. Chem. Int. Ed.* **2015**, *54*, 6795–6799; *Angew. Chem.* **2015**, *127*, 6899–6903; b) J. E. Mondloch, M. J. Katz, W. C. Isley III, P. Ghosh, P. Liao, W. Bury, G. W. Wagner, M. G. Hall, J. B. DeCoste, G. W. Peterson, R. Q. Snurr, C. J. Cramer, J. T. Hupp, O. K. Farha, *Nat. Mater.* **2015**, *14*, 512–516.
- [12] a) M. J. Katz, S.-Y. Moon, J. E. Mondloch, M. H. Beyzavi, C. J. Stephenson, J. T. Hupp, O. K. Farha, *Chem. Sci.* **2015**, *6*, 2286–2291; b) R. Gil-San-Millan, E. López-Maya, M. Hall, N. M. Padial, G. W. Peterson, J. B. DeCoste, L. M. Rodríguez-Albelo, J. E. Oltra, E. Barea, J. A. R. Navarro, *ACS Appl. Mater. Interfaces* **2017**, *9*, 23967–23973; c) T. Islamoglu, A. Atilgan,

- S.-Y. Moon, G. W. Peterson, J. B. DeCoste, M. Hall, J. T. Hupp, O. K. Farha, *Chem. Mater.* **2017**, *29*, 2672–2675.
- [13] G. W. Peterson, M. R. Destefano, S. J. Garibay, A. Ploskonka, M. McEntee, M. Hall, C. J. Karwacki, J. T. Hupp, O. K. Farha, *Chem. Eur. J.* **2017**, *23*, 15913–15916.
- [14] A. M. Plonka, Q. Wang, W. O. Gordon, A. Balboa, D. Troya, W. Guo, C. H. Sharp, S. D. Senanayake, J. R. Morris, C. L. Hill, A. I. Frenkel, *J. Am. Chem. Soc.* **2017**, *139*, 599–602.
- [15] K. M. Choi, K. Na, G. A. Somorjai, O. M. Yaghi, *J. Am. Chem. Soc.* **2015**, *137*, 7810–7816.
- [16] a) H. J. Park, J. K. Jang, S.-Y. Kim, J.-W. Ha, D. Moon, I.-N. Kang, Y.-S. Bae, S. Kim, D.-H. Hwang, *Inorg. Chem.* **2017**, *56*, 12098–12101; b) M. C. de Koning, M. van Grol, T. Breijjaert, *Inorg. Chem.* **2017**, *56*, 11804–11809.
- [17] J. C. Mareque-Rivas, R. T. M. de Rosales, S. Parsons, *Chem. Commun.* **2004**, 610–611.
- [18] a) G. Feng, J. C. Mareque-Rivas, R. T. M. de Rosales, N. H. Williams, *J. Am. Chem. Soc.* **2005**, *127*, 13470–13471; b) H. Linjalahti, G. Feng, J. C. Mareque-Rivas, S. Mikkola, N. H. Williams, *J. Am. Chem. Soc.* **2008**, *130*, 4232–4233; c) L. Lain, H. Lönnberg, T. Lönnberg, *Chem. Eur. J.* **2013**, *19*, 12424–12434; d) R. Bonomi, G. Saielli, U. Tonellato, P. Scrimin, F. Mancin, *J. Am. Chem. Soc.* **2009**, *131*, 11278–11279.
- [19] S. O. Odoh, C. J. Cramer, D. G. Truhlar, L. Gagliardi, *Chem. Rev.* **2015**, *115*, 6051–6111.
- [20] J. Hajek, M. Vandichel, B. Van de Voorde, B. Bueken, D. De Vos, M. Waroquier, V. Van Speybroeck, *J. Catal.* **2015**, *331*, 1–12.
- [21] J. E. Mondloch, W. Bury, D. Fairen-Jimenez, S. Kwon, E. J. DeMarco, M. H. Weston, A. A. Sarjeant, S. T. Nguyen, P. C. Stair, R. Q. Snurr, O. K. Farha, J. T. Hupp, *J. Am. Chem. Soc.* **2013**, *135*, 10294–10297.
- [22] H. Furukawa, F. Gándara, Y.-B. Zhang, J. Jiang, W. L. Queen, M. R. Hudson, O. M. Yaghi, *J. Am. Chem. Soc.* **2014**, *136*, 4369–4381.
- [23] I. Stassen, B. Bueken, H. Reinsch, J. F. M. Oudenhoven, D. Wouters, J. Hajek, V. Van Speybroeck, N. Stock, P. M. Vereecken, R. Van Schaijk, D. De Vos, R. Ameloot, *Chem. Sci.* **2016**, *7*, 5827–5832.
- [24] a) D. Troya, *J. Phys. Chem. C* **2016**, *120*, 29312–29323; b) G. Wang, C. Sharp, A. M. Plonka, Q. Wang, A. I. Frenkel, W. Guo, C. Hill, C. Smith, J. Kollar, D. Troya, J. R. Morris, *J. Phys. Chem. C* **2017**, *121*, 11261–11272.
- [25] L. Zhu, X.-Q. Liu, H.-L. Jiang, L.-B. Sun, *Chem. Rev.* **2017**, *117*, 8129–8176.
- [26] C. Caratelli, J. Hajek, F. G. Cirujano, M. Waroquier, F. X. L. i Xamena, V. Van Speybroeck, *J. Catal.* **2017**, *352*, 401–414.

Manuscript received: December 8, 2017

Accepted manuscript online: January 4, 2018

Version of record online: ■■■■■, ■■■■■, ■■■■■

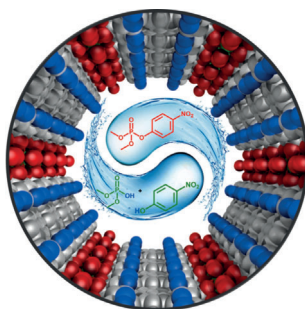
Communications



MOF Catalysts

T. Islamoglu, M. A. Ortuño,
E. Proussaloglou, A. J. Howarth,
N. A. Vermeulen, A. Atilgan, A. M. Asiri,
C. J. Cramer, O. K. Farha* — ■■■—■■■

Presence versus Proximity: The Role of
Pendant Amines in the Catalytic
Hydrolysis of a Nerve Agent Simulant



Proximity De-pendant: The role of amino groups on the hydrolysis of a nerve agent simulant, DMNP, has been explored. Experiments and theoretical calculations reveal that not only the presence but also the proximity of the amino group is important for effective chemical detoxification of DMNP. NU-1002-*o*-NH₂, a Zr-based mesoporous metal–organic framework (MOF) with pendant amines demonstrates $t_{1/2}$ of 1.2 min with only 3 mol% catalyst loading.